COPLANAR WAVEGUIDE DISCONTINUITIES FOR P-I-N DIODE SWITCHES AND FILTER APPLICATIONS

N.I. Dib, P.B. Katehi
Radiation Lab., University of Michigan, Ann Arbor, MI

G.E. Ponchak, R.N. Simons
NASA, Lewis Research Center, Cleveland, OH

ABSTRACT

A full wave space domain integral equation (SDIE) analysis of coplanar waveguide (CPW) two port discontinuities is presented. An experimental setup to measure the S-parameters of such discontinuities is described. Experimental and theoretical results for CPW realizations of pass-band and stop-band filters are presented. The S-parameters of such structures are plotted in the frequency range 5-25 GHz.

1 INTRODUCTION

The coplanar waveguide (CPW) was introduced for the first time in 1969 by C.P. Wen (1) as an appropriate transmission line for nonreciprocal gyromagnetic device applications. Recently, with the push to high frequencies and monolithic technology, CPWs have experienced a growing demand due to their appealing properties (2,3). However, the extent of applications of CPW circuits is limited due to the unavailability of circuit element models which can be incorporated into CAD programs. Houdart (2) proposed several configurations using the coplanar line technique in order to realize basic types of elements required in MIC's.

Microwave switches are circuit elements widely used in phase shifters and radiometers. A CPW switchable attenuating medium propagation, SAMP, switch has been demonstrated by Fleming *et al* (4). This device is useful for GaAs MMIC circuits but it is not easily incorporated into MIC's on passive substrates such as alumina or duroid. P-i-n diodes are good microwave switches since the impedance of the diode can be changed from a very high value to nearly zero in a short time. Recently, CPW p-i-n diode switches were proposed and fabricated (6). Fig.1 shows a switch were a diode is mounted across the open end of a quarter wavelength stub which is in series with the center strip conductor of the CPW. The two states of the switch, ON and OFF, can be realized separately by appropriate CPW discontinuities which in turn can be used to build pass-band and stop-band filters respectively (2,7,8).

In this paper, the space domain integral equation (SDIE) method, presented in (5), is extended to analyze the S-parameters of the CPW realization of the above switches, Fig.2. Experimental results are compared to theoretical data and a good agreement is achieved. The experimental setup, measurement technique and the sources of error are described. As a next step, the study of the switches will be completed by including the diode as a lumped element in the method of moments solution. Thus, the ON and OFF states of the switch will be predicted from the same structure without having to go to different CPW discontinuities for realization of these states.

2 THEORY

The coplanar line under consideration is shown in Fig.3. The measurements were performed using an open CPW structure. However, in the theoretical analysis the CPW is assumed to be inside a rectangular cavity of perfectly conducting walls as opposed to experiments where open structures were measured. The cavity dimensions were chosen such that the CPW fundamental mode is not affected by higher order cavity resonances.

The original boundary problem is split into two simpler ones by introducing an equivalent magnetic current $\bar{M}_s$ on the slot aperture. This surface magnetic current radiates an electromagnetic field in the two waveguide regions (above and below the slot) so that the continuity of the electric field on the surface of the slots is satisfied. The remaining boundary condition to be applied is the continuity of the tangential magnetic field on the surface of the slot apertures which leads to the following integral equation

$$\hat{n} \times \int_S \int [\bar{\bar{G}}_1^h - \bar{\bar{G}}_2^h] \cdot \bar{M}_s(\bar{r}')\, ds' = \bar{J}_s, \qquad (1)$$

where $\bar{\bar{G}}_{1,2}^h$ are the magnetic dyadic Green's functions in the two waveguide regions (5) and $\bar{J}_s$ denotes the ideal current source feeding the CPW, (gap generator model).

The integral equation (1) is solved using the method of moments where the unknown magnetic current is expanded in terms of rooftop basis functions. Then, Galerkin's method is applied to reduce the above equation to a linear system of equations

$$\begin{pmatrix} Y_{yy} & Y_{zy} \\ Y_{yz} & Y_{zz} \end{pmatrix} \begin{pmatrix} V_y \\ V_z \end{pmatrix} = \begin{pmatrix} I_y \\ I_z \end{pmatrix} \qquad (2)$$

where $Y_{ij}(i = y,z; j = y,z)$ represent blocks of the admittance matrix (5), V_i is the vector of unknown y and z magnetic current amplitudes, and I_j is the excitation vector which is identically zero everywhere except at the position of the sources. Finally, the equivalent magnetic current distribution and consequently the electric field in the slots are obtained by matrix inversion.

Away from the discontinuity, the slots fields form stand-

ing waves of the fundamental CPW propagating mode. Using the derived electric field , an ideal transmission line method as described in (9) is applied to determine the scattering parameters of the two port discontinuity.

3 EXPERIMENT

The circuits were fabricated using a liftoff procedure. A 2.8 μm gold layer was electron beam evaporated onto a 25 mil thick polished alumina substrate ($\epsilon_r = 9.9$). The alumina substrate was placed on a 125 mil thick 5880 RT/Duroid ($\epsilon_r = 2.2$) substrate with copper cladding on one side to serve as the bottom ground plane.

The RF measurements were performed using *HP8510* ANA and a probe station with design techniques $DC - 26\,GHz$ probes. In order to measure the circuit elements, an LRL calibration (10) was performed to remove the effects of the system to the reference plane PP' (Fig.4) using EEsof ANACAT software (11). The calibration standards shown in Fig.5 were fabricated on the same substrate as the cicuits.

4 RESULTS AND DISCUSSION

For the soluion of (2), most of the computation effort is spent on the evaluation of the elements of the admittance submatrices. These elements involve double summations in their computation which are inherently slowly convergent. Details on the numerical evaluation of these summations may be found in (12). Extensive numerical experiments were performed on the convergence of the S-parameters with respect to the above summations and the number of basis functions used in the expansion of the slot field. Both were chosen such that at least 2% accuracy is achieved.

Fig.6 shows the scattering parameters for the short circuit CPW stub (SC-CPW stub) of length 500 μm. It can be seen that the agreement between the theoretical and experimental results is very good. The differences can be due to conduction losses and radiation losses since an open structure was used in the measurements. Fig.7 shows the scattering parameters for the SC-CPW stub of length 1500 μm. From these results it can be observed that a resonance occures when the stub length is slightly less than a quarter wavelength ($\lambda_g \simeq 6.14mm$ at $f = 21\,GHz$). This is due to the inductive reactance which exists at the end of the stub as a result of the end effect. A stop-band filter can be realized by cascading several SC-CPW stubs in series.

Figs.8 and 9 show the scattering parameters for the open circuit CPW stub (OC-CPW stub) of length 500 μm and 1500 μm respectively. It can be seen from Fig.9 that S_{11} (S_{12}) has its minimum (maximum) value at $f = 19\,GHz$ at which $\lambda_g/4 \simeq 1.7mm$. This is due to the capacitive end effect of the stub. Such structures operate as pass-band filters. The agreement between the theoretical and experimental results is very good.

The errors associated with the measured data are nonrepeatability in probe placement and pressure and circuit fabrication tolerances. The circuit dimension variations across the $2in. \times 2in.$ alumina substrate were negligible as was the variation in the gold thickness. The circuit dimensions varied by, at most, 1% compared to the designed dimensions. The probe placement was repeatable to 5 μm. The probe pressure created the largest uncertainty in the measurements since it changed the contact between the alumina and the duroid substrates. One further consideration is that the spacing between circuits on the substrate was approximately $(S + 2W)/2$ which resulted in a finite size ground planes.

5 CONCLUSIONS

The space domain integral equation method solved by the method of moments (Galerkin's technique) in conjunction with simple transmission line theory was applied to analyze CPW realizations of pass-band and stop-band filters. An experimental setup to measure the S-parameters of those structures has been described and the various sources of error were discussed. The agreement between the theoretical data and the experimental measurements was very good, thus, the validity of both results is verified.

6 ACKNOWLEDGMENT

The theoretical part of this paper was supported by the National Science Foundation under contract ECS-8657951.

References

[1] C.P. Wen, "Coplanar Waveguide: A Surface Strip Transmission Line for Nonreciprocal Gyromagnetic Device Applications," *IEEE Trans. on Microwave Theory and Techniques*, Vol. MTT-17, pp.1087-1090, Dec.1969.

[2] M. Houdart, "Coplanar Lines: Application to Broadband Microwave Integrated circuits," *Proc. of 6th European Microwave Conference (Rome)*, pp.49-53, 1976.

[3] K.C. Gupta, R. Garge and I.J. Bahl, *Microstrip Lines and Slotlines*, Dedham, MA: Artech House, 1979.

[4] P.L. Fleming, T. Smith, H.E. Carlson, and W.A. Cox, "GaAs SAMP Device for Ku-Band Switching," *IEEE Trans. on Microwave Theory and Techniques*, Vol. MTT-27, pp.1032-1035, 1979.

[5] N.I. Dib and P.B. Katehi, "Modeling of Shielded CPW Discontinuities Using the Space Domain Integral Equation Method (SDIE)," *submitted to JEWA, Special Issue on Electromagnetism and Semiconductors.*

[6] G.E. Ponchack and R.N. Simons, "Channelized Coplanar Waveguide PIN-Diode Switches," *19th European Microwave Symposium Digest (London)*, pp.489-494, 1989.

[7] R.N. Bates, "Design of Microstrip Spur-Line Band-Stop Filters," *IEE Trans. Microwaves, Optics and Acoustics*, Vol.1, No.6, pp.209-214, Nov.1977.

[8] D.F. Williams and S.E. Schwarz, "Design and Performance of Coplanar Waveguide Band-Pass Filters," *IEEE Trans. on Microwave Theory and Techniques*, Vol. MTT-31, pp.558-566, July 1983.

[9] P.B. Katehi, "A Generalized Method for the Evaluation of Mutual Coupling in Microstrip Arrays," *IEEE Trans. on Antennas and Propagation*, Vol. AP-35, pp.125-133, Feb.1987.

[10] P.R. Pantoja, M.J. Howes, J.R. Richardson, and R.D. Pollard, "Improved Calibration and Measurement of the Scattering Parameters of Microwave Integrated Circuits," *IEEE Trans. on Microwave Theory and Techniques*, Vol. MTT-37, pp.1675-1680, Nov.1989.

[11] EEsof Inc., -Anacat Users Manual.

[12] L.P. Dunleavy and P.B. Katehi, "Generalized Method for Analyzing Shielded Thin Microstrip Discontinuities," *IEEE Trans. on Microwave Theory and Techniques*, Vol. MTT-36, pp.1758-1766, Dec.1988.

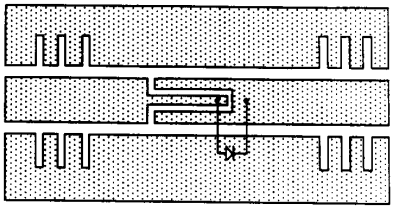

Figure 1: Schematic diagram of CPW p-i-n diode switched series-stub switch.

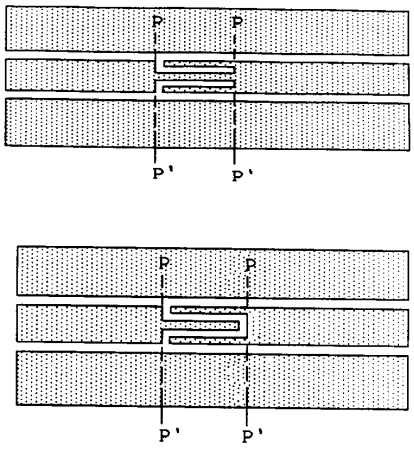

Figure 2: CPW realizations of stop-band and pass-band filters.

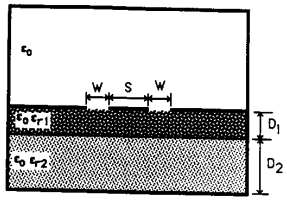

Figure 3: A coplanar waveguide inside a cavity.

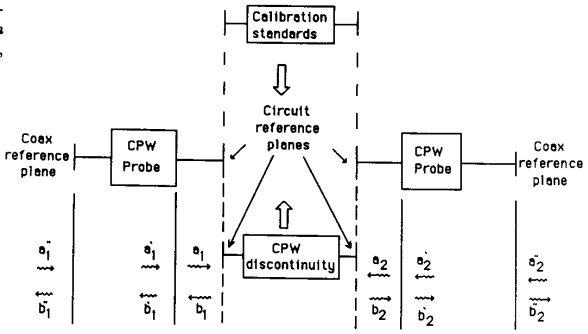

Figure 4: Basic concept of de-embeding.

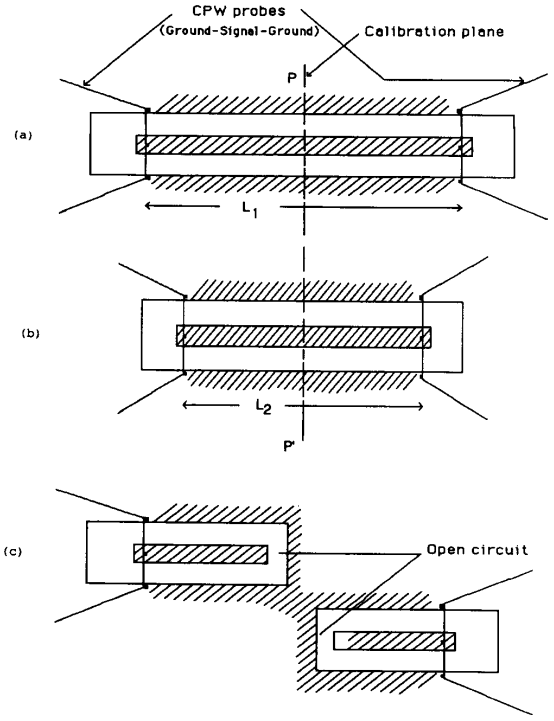

Figure 5: CPW standards for LRL calibration: (a) Delay of length L_1, (b) Delay of length L_2, (c) Reflection of arbitrary magnitude.

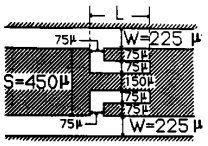

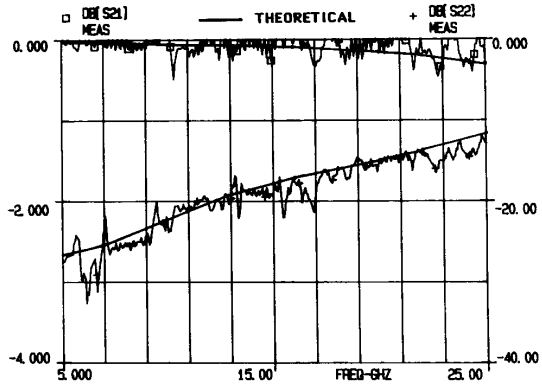

Figure 6: S-parameters for SC-CPW stub with L=500 μm, ($D_1 = 25mil, D_2 = 125mil, \epsilon_{r1} = 9.9, \epsilon_{r2} = 2.2$).

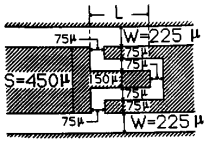

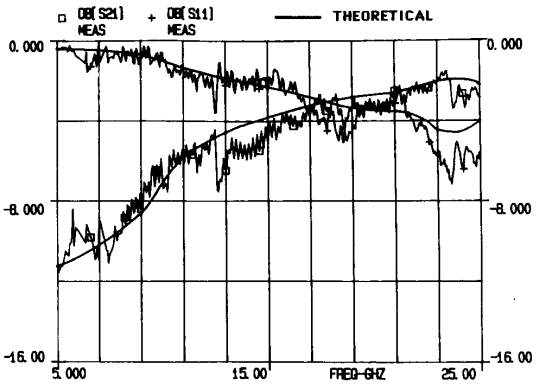

Figure 8: S-parameters for OC-CPW stub with L=500 μm, ($D_1 = 25mil, D_2 = 125mil, \epsilon_{r1} = 9.9, \epsilon_{r2} = 2.2$).

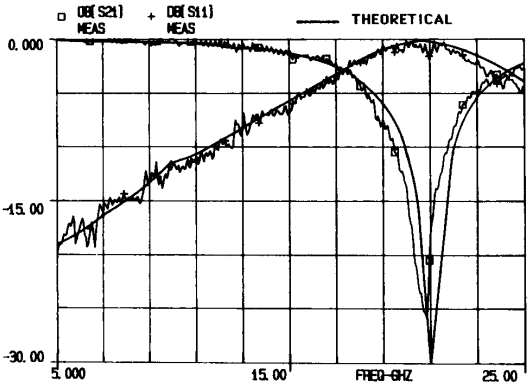

Figure 7: S-parameters for SC-CPW stub with L=1500 μm, (Other dimensions are the same as in Fig.6).

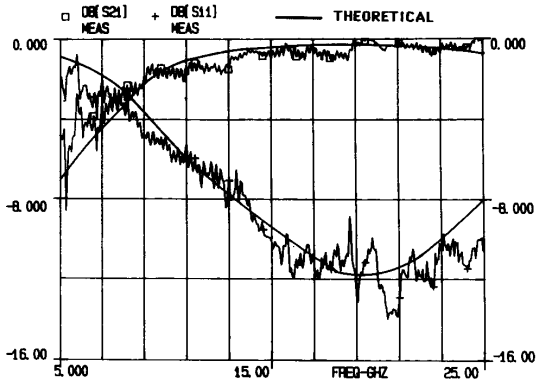

Figure 9: S-parameters for OC-CPW stub with L=1500 μm, (Other dimensions are the same as in Fig.8).